SEMARAK ILMU PUBLISHING

Journal of Advanced Research in Fluid Mechanics and Thermal Sciences

Journal homepage:
https://semarakilmu.com.my/journals/index.php/fluid_mechanics_thermal_sciences/index
ISSN: 2289-7879

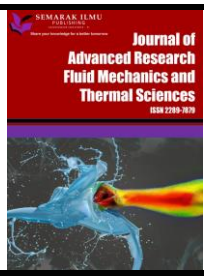

Numerical Simulation of Ventilation in a Confined Space

Lam Wai Kit[1,*], Hassan Mohamed[1,2], Ng Yee Luon[1], Leon Chan[3]

[1] College of Engineering, Department of Mechanical Engineering, Universiti Tenaga Nasional, 43000 Kajang, Selangor, Malaysia
[2] Institute of Sustainable Energy, Universiti Tenaga Nasional, Jalan Ikram - Uniten, 43000 Kajang, Selangor, Malaysia
[3] Department of Mechanical Engineering, University of Melbourne, Parkville, VIC 3010, Australia

ARTICLE INFO

Article history:
Received 20 January 2023
Received in revised form 19 May 2023
Accepted 25 May 2023
Available online 13 June 2023

Keywords:
Numerical simulation; ventilation; room temperature; energy

ABSTRACT

Numerical simulation of ventilation in a confined space is conducted with different quantities of heat sources and various conditions of the room with a constant ambient temperature of 298K. The velocity streamline plot shows a different air recirculating pattern in the case with the air ventilation system switched off. The room with an extreme condition achieves the highest temperature of T=310K. The lowest temperature is obtained in the case with a relaxing condition where $T=T_{ac}$=294K. The efficiency of systems reduces when the air conditioner and air ventilation system operate at the same time. The efficiency of the air conditioner increases, and the ambient temperature achieves minimum value when the air ventilation system remains off. The position of the air conditioner is closed to the air ventilation system causing the efficiency of the system to reduce. This is due to the air ventilation system drawing cold air out of the room before convective heat transfer occurs.

1. Introduction

Thermal comfort and energy efficiency are crucial to the design of engineering laboratory such as heat transfer from the machine to the surrounding. Thermal comfort is defined as the condition of mind that expresses satisfaction with the thermal environment [1]. It is also known as a condition for someone is not feeling either too cold or too warm. Thermal comfort is not only a potential health hazard but also an impact on a people to function efficiently and effectively. The cause of thermal comfort failure is categorized to environmental and personal factors (personal factors are not covered in current study). Three main components that have high impact to the thermal comfort are the air flow (velocity of the air), human body or surrounding temperature and relative humidity (RH). Muhieldeen and Kuang [2] conducted experimental and numerical study to investigate energy and cost savings in a building. The result shows the percentage of energy saving able to be achieved with increasing air temperature using greater air flow. The predicted mean vote (PMV) values of building occupants decrease as increasing the air flow in the building with the least predicted percentage of dissatisfied (PPD).

* *Corresponding author.*
E-mail address: k3ithkit@gmail.com

https://doi.org/10.37934/arfmts.107.1.118

The characteristic of air flow is important to achieve human comfort temperature and well-being of an individual. Nielsen *et al.,* [3,4] conducted experimental and numerical study to investigate the velocity flow field in the modelled room with different geometric arrangement for isothermal condition and with a heating floor [3-5]. Numerical calculation shows a good agreement with experimental results. Daoud and Galanis [6] conducted three-dimensional numerical simulation using Zonal model and had a good agreement with experimental results from Nielsen *et al.,* [5]. Omri and Galanis [7] conducted numerical simulation using Fluent with three different turbulence models namely k - ε, RNG k - ε and k -ω SST. The result is validated with ventilated isothermal cavity cases from Nielsen *et al.,* [4,5]. RNG k - ε and k - ω SST models show a good agreement while k - ε model overestimates the thickness of jet. Zhang *et al.,* [8] perform numerical simulations with a total of eight turbulence models to investigate the airflow and turbulence in an enclosed environment. The simulation result is compared with experimental results from literature. RNG k - ε model shows the best performance compares to other turbulence models in terms of accuracy, computational efficiency and robustness.

The indoor air quality (IAQ) and thermal comfort in a room or building has been widely studied. Zhu *et al.,* [9] conducted numerical study using ANSYS to investigate the flow field and heat transfer around the building to enhance the indoor thermal environment and thermal efficiency at a rural area in Ningxia, China. The efficiency of system is evaluated using local mean age such as forced ventilation inside food plants and naturally ventilated office [10,11]. An investigation of thermal comfort is carried out to study the turbulent mixed convection in an indoor ventilated ice rink. Benderradji *et al.,* [12] conducted three-dimensional incompressible flow of mixed convection simulation with different Reynolds and Grashof numbers to investigate the air flow in a cavity. They reported the flow regime is strongly dependent on both Grashrof and Reynolds numbers. Some other studies have been carried out to investigate the air ventilation of an indoor atrium space or badminton hall [16,17].

A rectangular cavity is commonly used in laboratory experiment or numerical simulation to study the air flow in a modelled room. The study may predict the velocity characteristics in a room, but the statistics are not applicable for a laboratory with two operating Capstone C30 micro gas turbine which generates a large amount of heat to the surrounding. The purpose of this study is to investigate the pattern of the air flow and heat transfer in the room with different quantity of heat source. This is to determine if the room temperature is comfortable for occupant. Various condition of the room has been simulated and the analysis of simulation will be presented in section 3.

2. Numerical Methodology

2.1 Governing Equation

The simulations were simulated using OpenFOAM [13] with the *buoyantPimpleFoam* solver with the k - ε turbulence model. The *buoyantPimpleFoam* solver is selected for the parametric study as large temperature difference results in density variations in the simulation case. It is a transient solver for buoyant, turbulent flow of compressible fluids for ventilation and heat transfer and the density is solved using the ideal gas equation in Eq. (4) [14]. The governing equations employed in the study take the form

$$\frac{\partial \rho}{\partial t} + \nabla \cdot (\rho \mathbf{u}) = 0 \tag{1}$$

$$\frac{\partial \rho}{\partial t} + \nabla \cdot (\rho \mathbf{u}\mathbf{u}) = -\nabla p + \rho g + \nabla \cdot (2\upsilon_{eff} D(\mathbf{u})) - \nabla(\frac{2}{3}\nu_{eff}(\nabla \cdot \mathbf{u})) \tag{2}$$

$$\frac{\partial(\rho h)}{\partial t} + \nabla \cdot (\rho \mathbf{u} h) = \frac{\partial \rho \mathbf{K}}{\partial \mathbf{t}} + \nabla \cdot (\rho \mathbf{u} K) - \frac{\partial \rho}{\partial t} = \nabla \cdot (\alpha_{eff} \nabla h) + \rho \mathbf{u} \cdot g \quad (3)$$

$$\rho = \frac{p}{RT} \quad (4)$$

where the ρ is the density of the fluid and ***u*** is the velocity vector. *p* is the pressure and *g* is the unit vector for the direction of gravity. The effective viscosity, v_{eff} is the sum of the molecular and turbulent viscosity. $D(\mathbf{u})$ is the strain rate tensor and is defined as $D(\mathbf{u}) = 1/2(\nabla \mathbf{u} + (\nabla \mathbf{u})^T)$. *h* is the enthalpy per unit mass and $K = |u|^2/2$ is the kinetic energy per unit mass. α_{eff} is the thermal effective diffusivity and is the sum of the laminar and turbulent thermal diffusivities. *R* is the specific gas constant and *T* is the temperature of the fluid.

2.2 Test Case Validation

The *buoyantPimpleFoam* (BPF) solver is validated with a test case from Nielsen *et al.,* [3] and Limane *et al.,* [15]. The schematic of the rectangular cavity that used to validate the OpenFOAM code is shown in Figure 1. The three-dimensional cavity has the wall-normal height, H = 127mm, streamwise length, L = 3H and spanwise length W = 4.7H. The fresh is enter from an inlet with the height, h = 0.056H where it is located at the top-left side (z = 0) and exit through an outlet with the height, t = 0.16H at the bottom-right side (z = L). No slip boundary condition is employed to the front-back walls, side walls along with ceiling and floor.

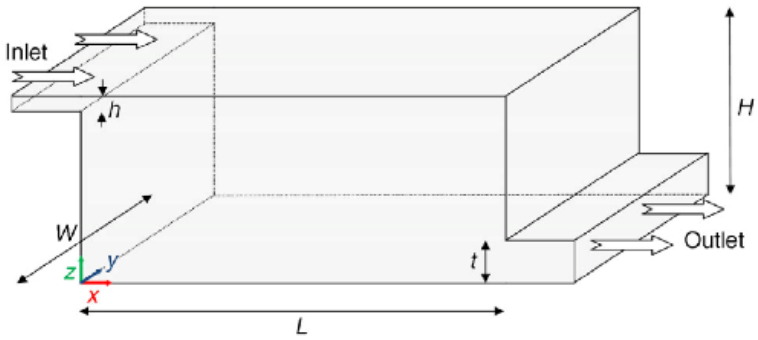

Fig. 1. Schematic of the cavity test case [3,15]

The fresh air with a speed of U_0 = 15.2m/s is introduced with the turbulence intensity of 5% ($U' = 0.05U_0$) and a temperature of 295.15K. The Reynolds number is fixed at Re = 7100 for all cases. All the walls are considered adiabatic for all the simulation case expect the floor where a uniform heat flux q = 563W/m2 (or Q = 128W) is applied to the floor. The computational grid domain is equally spaced with the size of N_x, N_y and N_z of 92 × 94 × 48. The Courant number is set at maximum of 0.5 to ensure the numerical stability and increase the accuracy of the simulation.

Figure 2 shows the normalized velocity distribution along the cavity height with x = 2H and y = W/2. The negative velocity shows the presence of recirculating air at that area. The velocity plot shows a good agreement with experimental result from Nielsen [3] and simulation result from Limane *et al.,* [15]. However, deviation can be observed in the plot of the normalized temperature profile along two horizontal lines with y = 0.67W and z = 0.25H (see Figure 2). Current result overestimates the temperature compared to both experimental and simulation results.

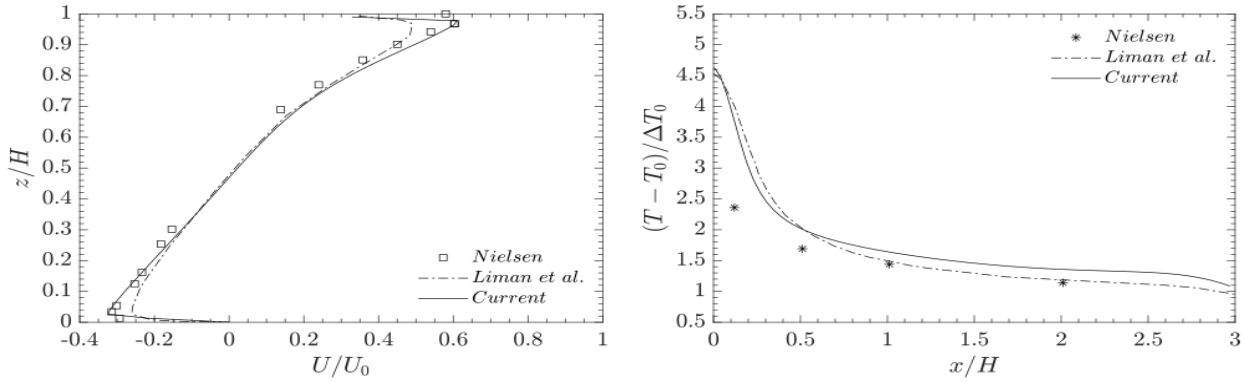

(a) (b)

Fig. 2. Plot of the normalised (a) Velocity (b) Temperature compare with previous studies [3,4]

2.3 Parametric Study

Figure 3 shows the three-dimensional model of the room with the dimension of 8m × 5.3m × 2.9m ($L_x \times L_z \times L_y$) with an ambient temperature of 298K. Two Capstone C30 with the dimension of 0.8m × 1.5m × 1.8m ($l_x \times l_z \times l_y$) is represented by a heat source. Two heat sources are installed on both sides of the room with a constant temperate of 328K when it is operating. Two air ventilation with the size of 0.5m x 0.5m is installed on top of each heat source and is shown in Figure 3(b). The air ventilation system draws the hot air out of the room with a speed of 1.4m/s. The air-conditioning system with the volumetric flow rate of 0.35m^3/s has the outer length (a_o) of 0.5m with internal length (a_i) of 0.3 and the internal surface is set to be a wall. No slip boundary condition is applied to all sides of the wall. The computational grid domain is equally spaced with the size of N_x, N_y and N_z of 80 x 29 x 53.

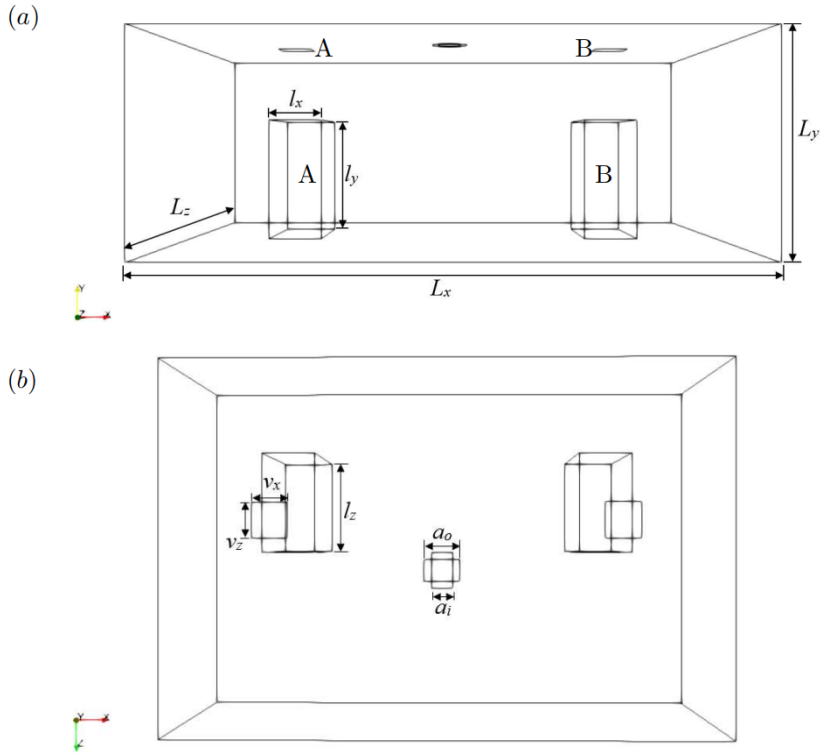

Fig. 3. 3D model of the room in (a) Side view (b) Top view

2.4 Grid Independent Study

The comparison of velocity streamline contour plot with different mesh size is shown in this section. No refinement done throughout the domain in Figure 4(a) and Figure 5(a) and refinement is applied to the whole computational domain in Figure 4(b) and Figure 5(b). The cells are divided in streamwise (*x*), wall-normal (*y*) and spanwise (*z*) direction and resulting eight times the number of cells. Case 4 is selected for grid independent study as the condition is extreme where all the heat sources, air ventilation and air-conditioner are turned on. With the extreme set-up, we can know if the mesh is sufficiently resolving all the required parameters.

Figure 4 shows velocity streamlines on the temperature contour. Maximum positive U_y=*1m/s* is observed at the centre of air ventilation system where the air is drawn out of the room vertically. Multiple air recirculation can be observed in both the contours. The significant difference between both the contours are the air flow pattern around the heat source. Streamlines for the case with no refinement show that the air is flowing towards the heat source. However, the air flow in 4(b) is flowing away from the heat source.

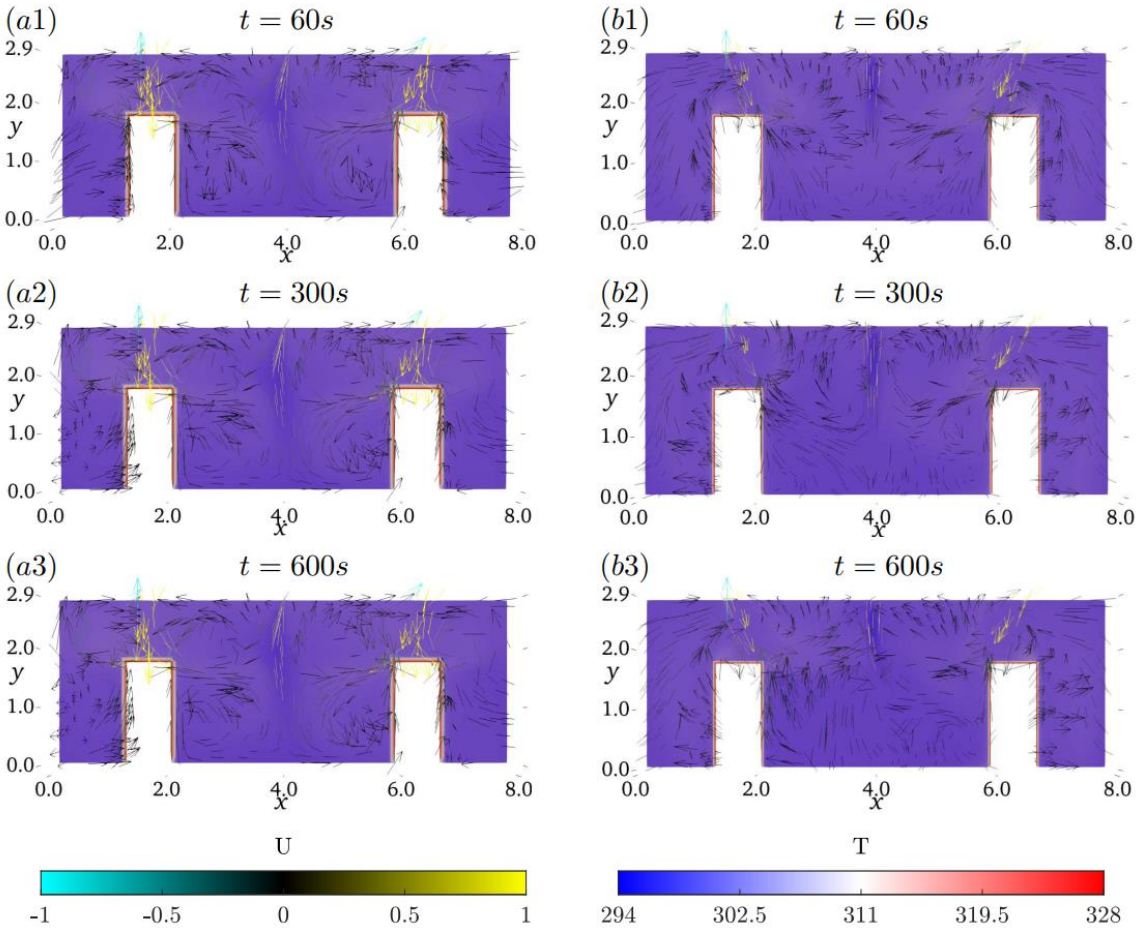

Fig. 4. Slice of temperature contour at L_z = 2.25m with velocity streamlines for Case 4 at respective time for (a) No refinement (b) Refinement

The *x* - *z* plane temperature contour in Figure 4(a) differ significantly compares to Figure 4(b). The case without refinement overestimates the temperature around the heat source. Velocity streamlines plot coloured by temperature is shown in Figure 5. Streamlines in Figure 5(a) are significantly different compared to the streamline in Figure 5(b). The ambient temperature on the

other hand is similar in both the cases where T ≤ 302K. Based on the streamlines plot, we can capture more flow patterns and accurate flow statistics. In this study, the refinement grid is selected to ensure the simulation able to capture accurate flow statistics and temperature field around the room.

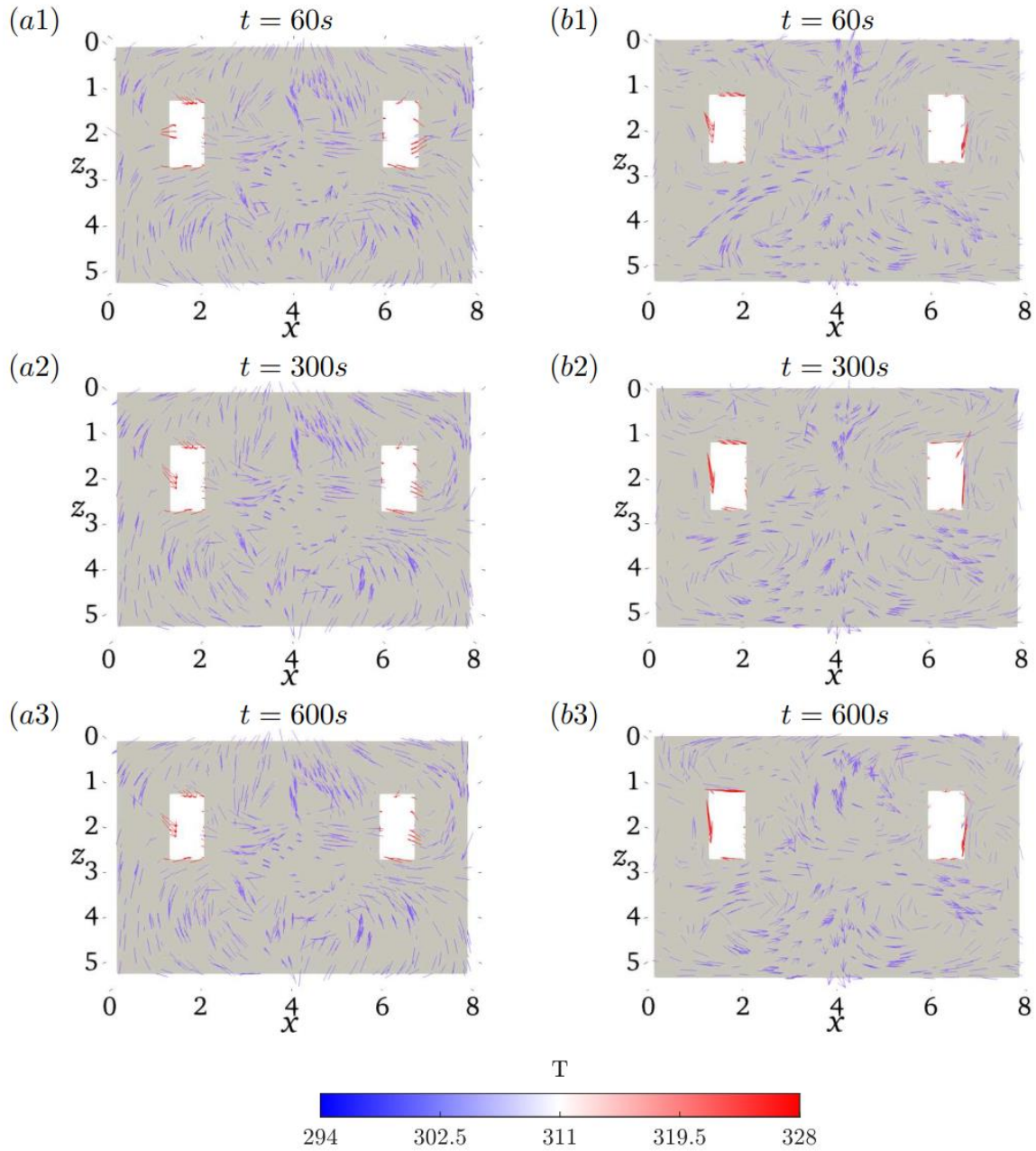

Fig. 5. Slice of velocity streamlines plot at L_y = 1.5m coloured by temperature for Case 4 at respective time, t at (a) No refinement (b) Refinement

3. Result and Discussion

Total of 6 cases are simulated with various condition where the condition of air conditioner and air ventilation system are manipulated and shown in Figure 3. The boundary condition of the simulation is changing respectively with room condition. The simulation covers room condition from relax (heat sources and air ventilation system is turned off, but the air conditioner is operating) to

extreme condition (heat sources and air ventilation system is operating but the air-conditioner is switched off) to study the relationship between airflow and heat transfer.

Table 1 shows the details of the cases with various room conditions in this study. Cases 0 and 3 represent the relax and extreme conditions. Cases 1 and 4 have different numbers of heat sources with an operating air-conditioner and ventilation system, while cases 2 and 5 have only an air-conditioner operating.

Table 1
Different room condition for the simulation

Cases	Gas Turb. A	Gas Turb. B	Air Vent A	Air Vent B	Air Cond.
0	Off	Off	Off	Off	On (T_{ac}=294K)
1	On	Off	On	On	On (T_{ac}=294K)
2	On	Off	Off	Off	On (T_{ac}=294K)
3	On	On	On	On	Off
4	On	On	On	On	On (T_{ac}=294K)
5	On	On	Off	Off	On (T_{ac}=294K)

3.1 Effect of Heat Source(s)

In this section, the result of simulations is discussed by comparing the velocity streamlines and ambient temperature under different room condition quantity of heat source. The velocity in wall-normal direction, U_y is rescaled to the range between -1 and 1. Negative velocity indicates the air is recirculating or drawn out of the room.

Figure 6 shows the temperature contour with velocity streamlines for Case 1 and 4. Maximum negative U_y is observed at the centre of the air ventilation system where the air is drawn out of the room vertically. Cold air is released from the air conditioner (located at the centre of the contour) has a maximum positive U_y. Multiple air recirculation can be observed in the midst of plot. Case 4 has a higher temperature compared to Case 1 where two heat sources are enabled. Heat convection occurs and increases the temperature around heat sources.

Velocity streamlines plot coloured by temperature is plotted at the wall-normal height, L_y = 1.5m (where it is the chest height of occupant). This allow the investigation of determining if the room temperature is comfortable for occupant. Lowest temperature region is found located at the left side in Figure 7(a) where only a heat source is enabled at the right side with the operating temperature of 328K. The colour in Figure 7(b) is fading from blue to light blue indicates temperature is rising. The colour of the contour in Case 1 is significantly darker compared to Case 4 indicates temperature is lower. This is due to only a heat source is enabled in Case 1, but two heat sources are enabled in Case 4. The ambient temperature reaches constant at T ≤ 298K and T ≤ 302K for Case 1 and 4 at t = 600s in Figure 7(a3) and Figure 7(b3) respectively.

Figure 8 shows the temperature contour with velocity streamlines for Case 2 and 5. The air ventilation system is switched off in these simulations and the boundary condition is set to *inletOutlet*. Maximum negative U_y is observed at the air vent where the air is flowing out of the room. Maximum positive U_y is occurred at the center in Figure 8(a) and Figure 8(b) are the air flow from the air conditioner in the spanwise direction, z. Recirculation of air is observed in the center of plot. It is worth noting that different air recirculation pattern is observed in the midst of the contour when air ventilation system is switched off. The temperature in Case 3 is higher than Case 0 where multiple heat sources are enabled.

Velocity streamlines plot coloured by temperature for Case 2 and Case 5 are shown in Figure 9(a) and Figure 9(b) respectively. The contour becomes darker in colour from t = 60s to t = 300s indicates

the temperature is decreasing in Figure 9(a1) and Figure 9(a2) respectively. The contour in Figure 9(a3) is significantly darker compares to Figure 9(b3). This indicates Case 2 has a lower ambient temperature compared to Case 5 at t = 600s where only a heat source is enabled.

The room is compared from relax to extreme condition. For relax condition (see Figure 10(a)), heat sources and air ventilation system are switched off. Air conditioner is set to be on in Case 3 (see Figure 10(b)) to prevent simulation error where the room become a vacuum chamber when no air is supplied from inlet. Maximum positive U_y is observed at the centre of air ventilation system. Cold air releases from air conditioner have maximum negative U_y. Both the cases have a significant different pattern of air flow. The temperature of cold air is set to be 298K (equivalent to ambient temperature) to increase the accuracy of simulation in Case 3. In Figure 11(a), the ambient temperature is decreased and reached constant at t = 300s where T = Tac = 294K (see Figure 11(a2)). The colour contour in Figure 11(b) is faded from blue to light-blue and the temperature increases to 305K in Figure 9(b2) and Figure 9(b3) respectively.

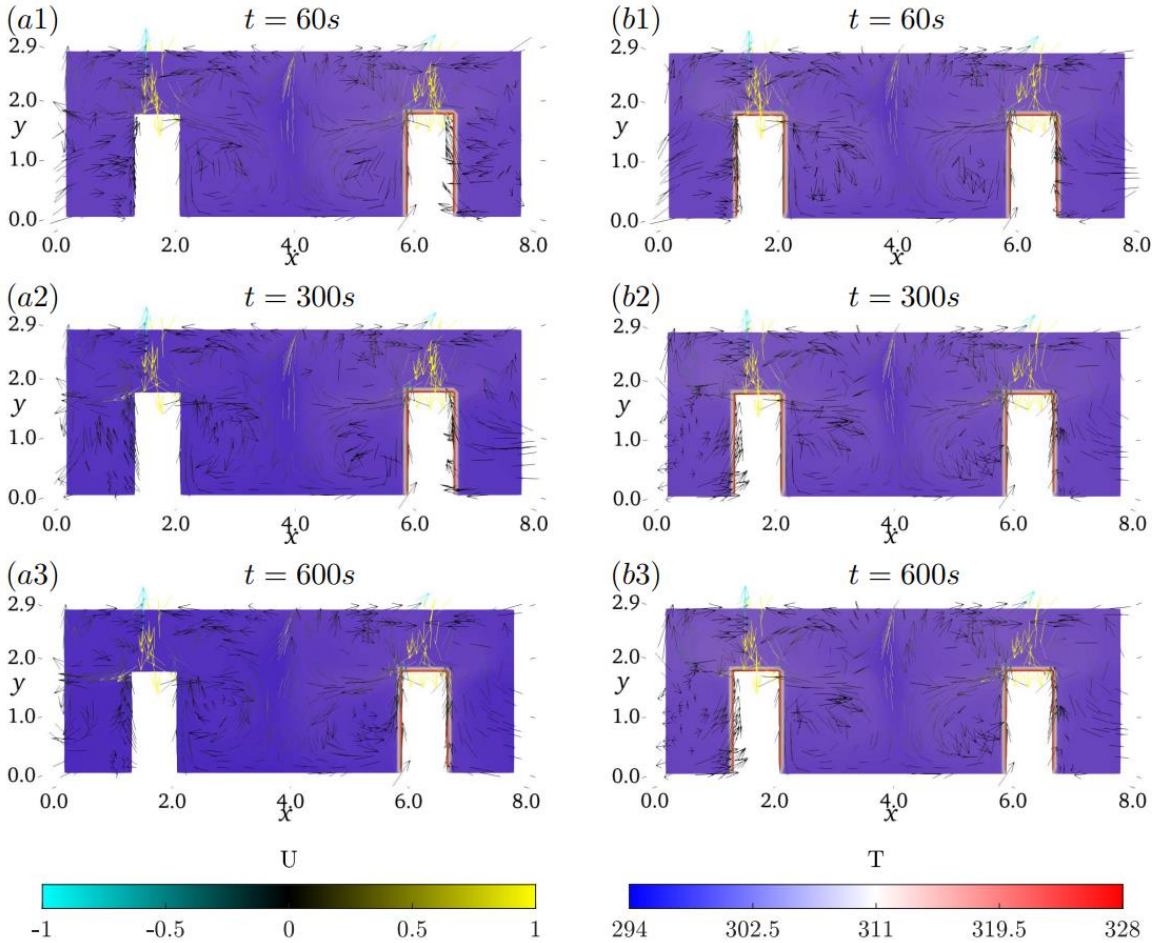

Fig. 6. Slice of temperature contour at L_z = 2.25m with velocity streamlines for Case 4 at respective time, t for (a) Case 1 (b) Case 4

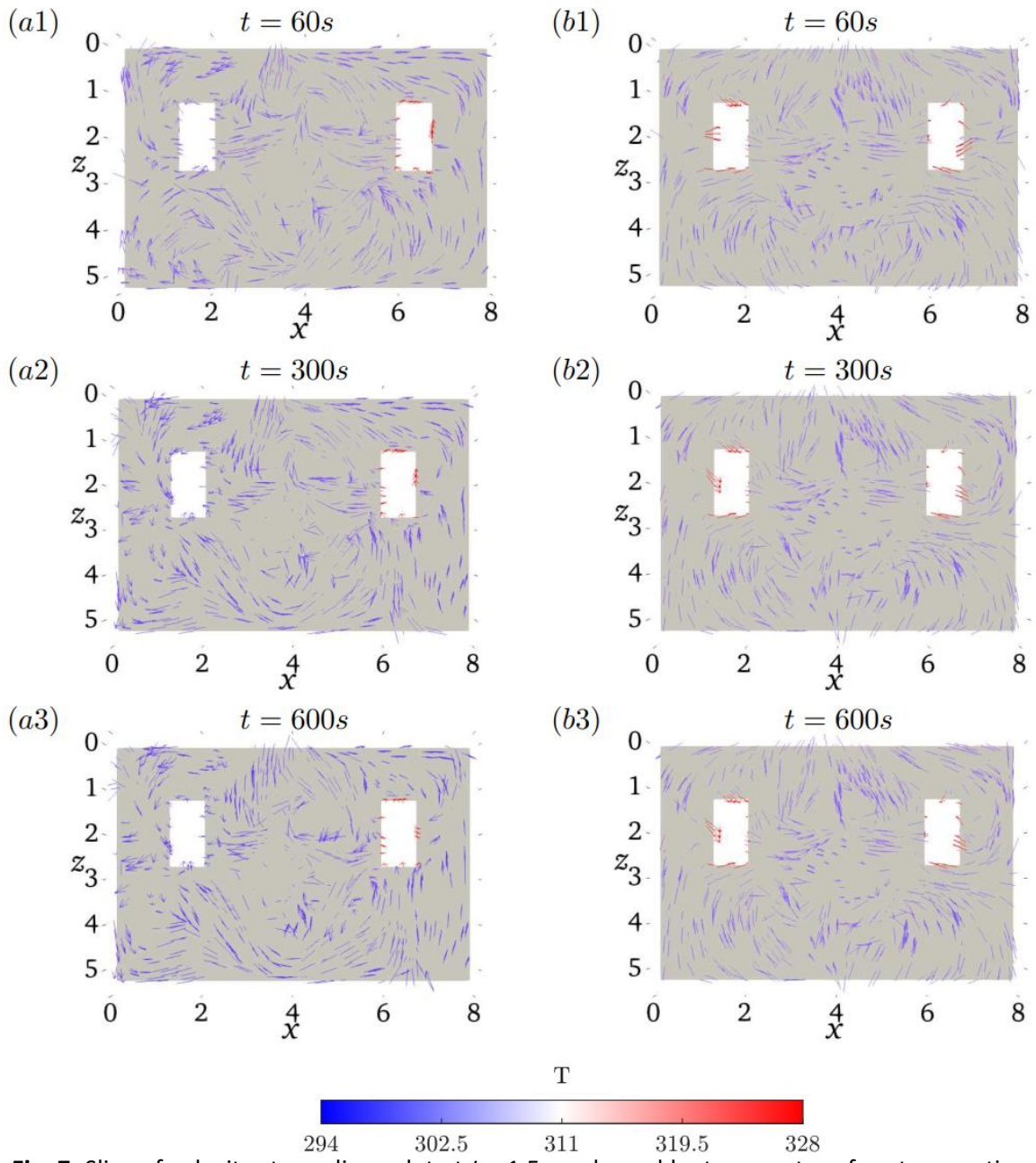

Fig. 7. Slice of velocity streamlines plot at L_y = 1.5m coloured by temperature for at respective time, t for (a) Case 1 (b) Case 4

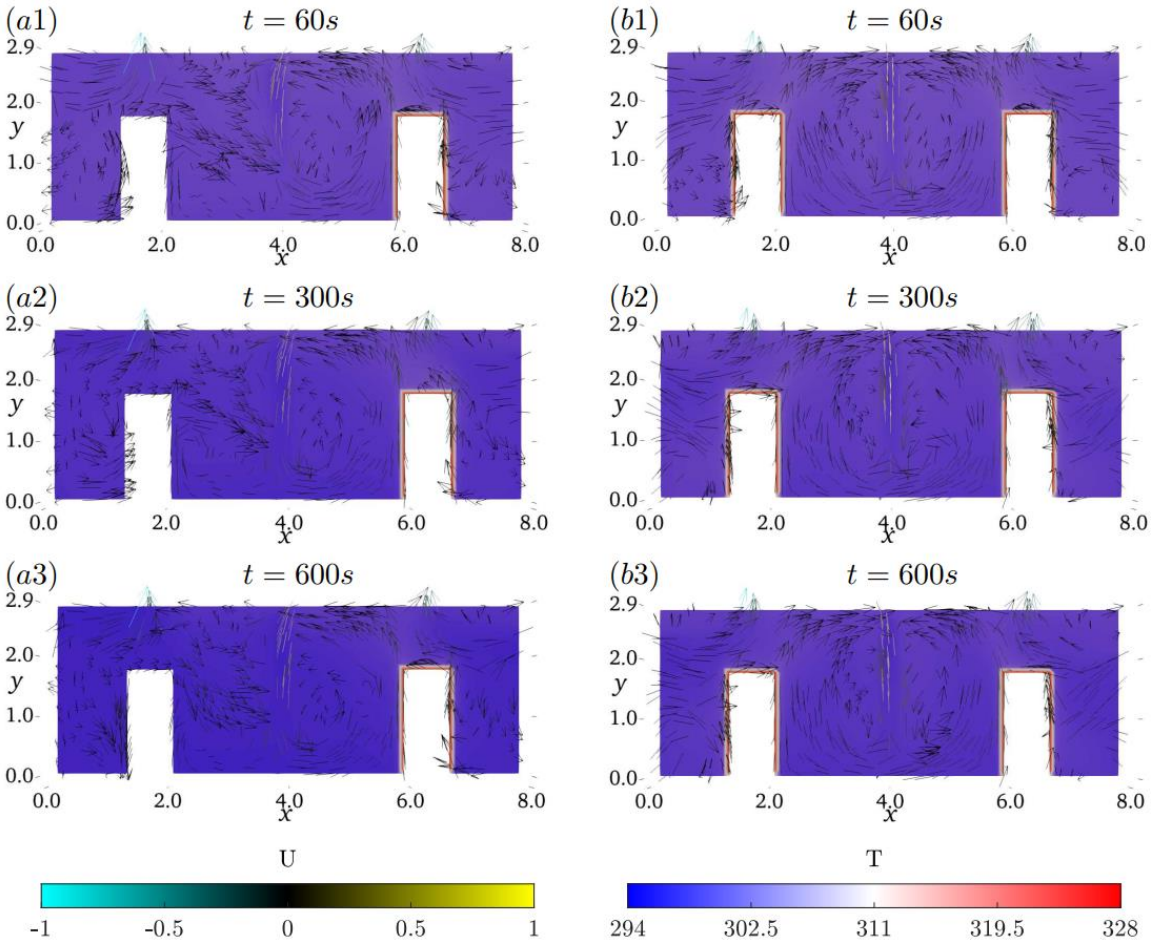

Fig. 8. Slice of temperature contour at L_z = 2.25m with velocity streamlines for Case 4 at respective time for (a) Case 2 (b) Case 5

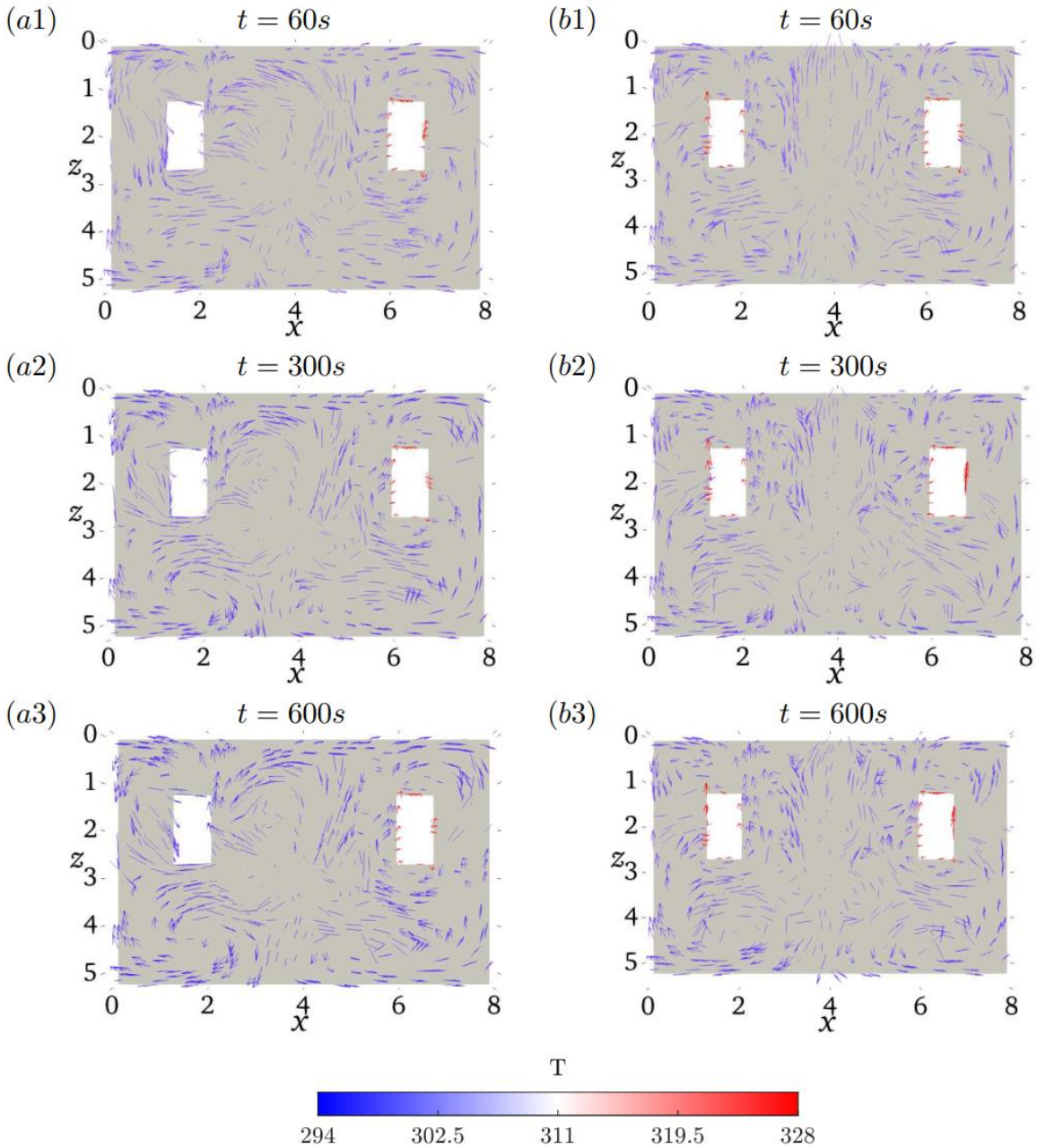

Fig. 9. Slice of velocity streamlines plot at L_y = 1.5m coloured by temperature for at respective time, t for (a) Case 2 (b) Case 5

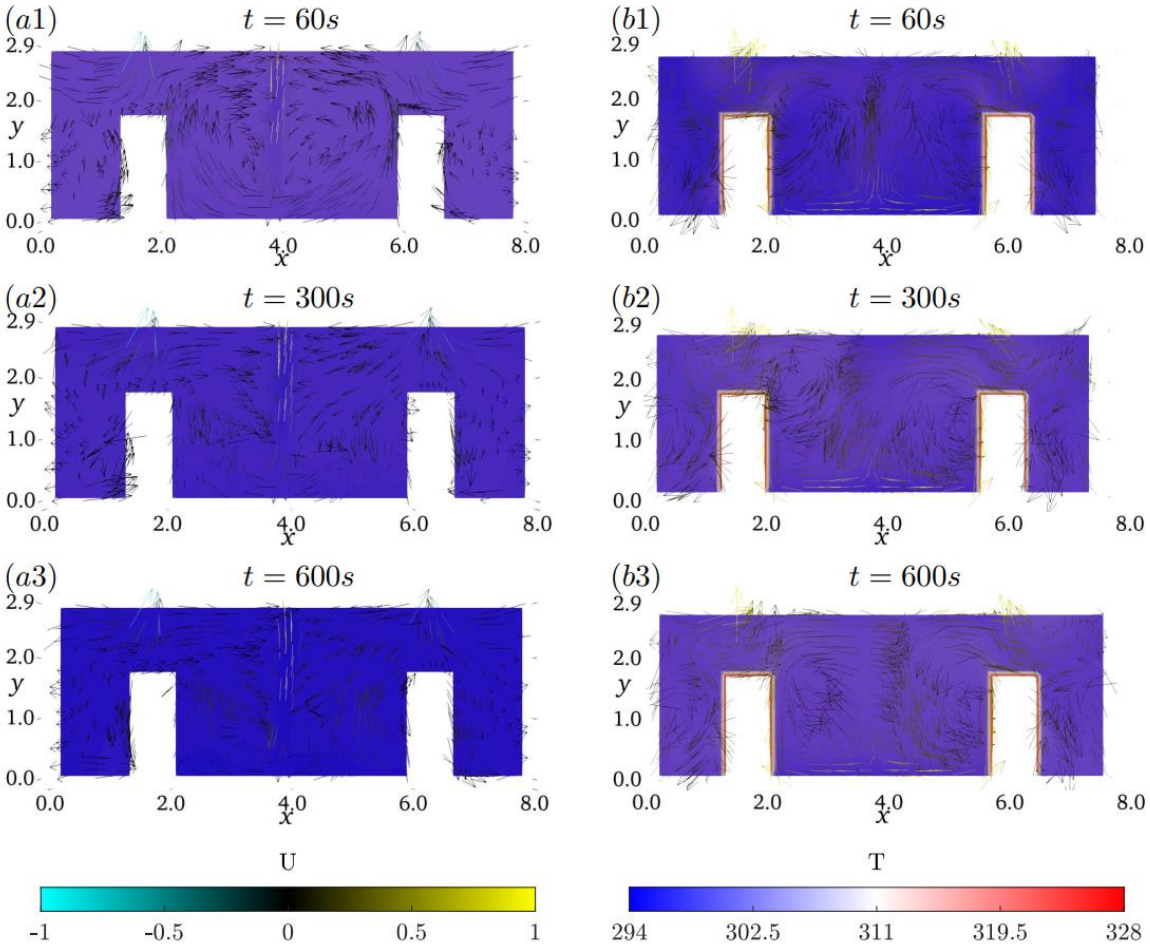

Fig. 10. Slice of temperature contour at L_z = 2.25m with velocity streamlines for Case 4 at respective time, t for (a) Case 0 (b) Case 3

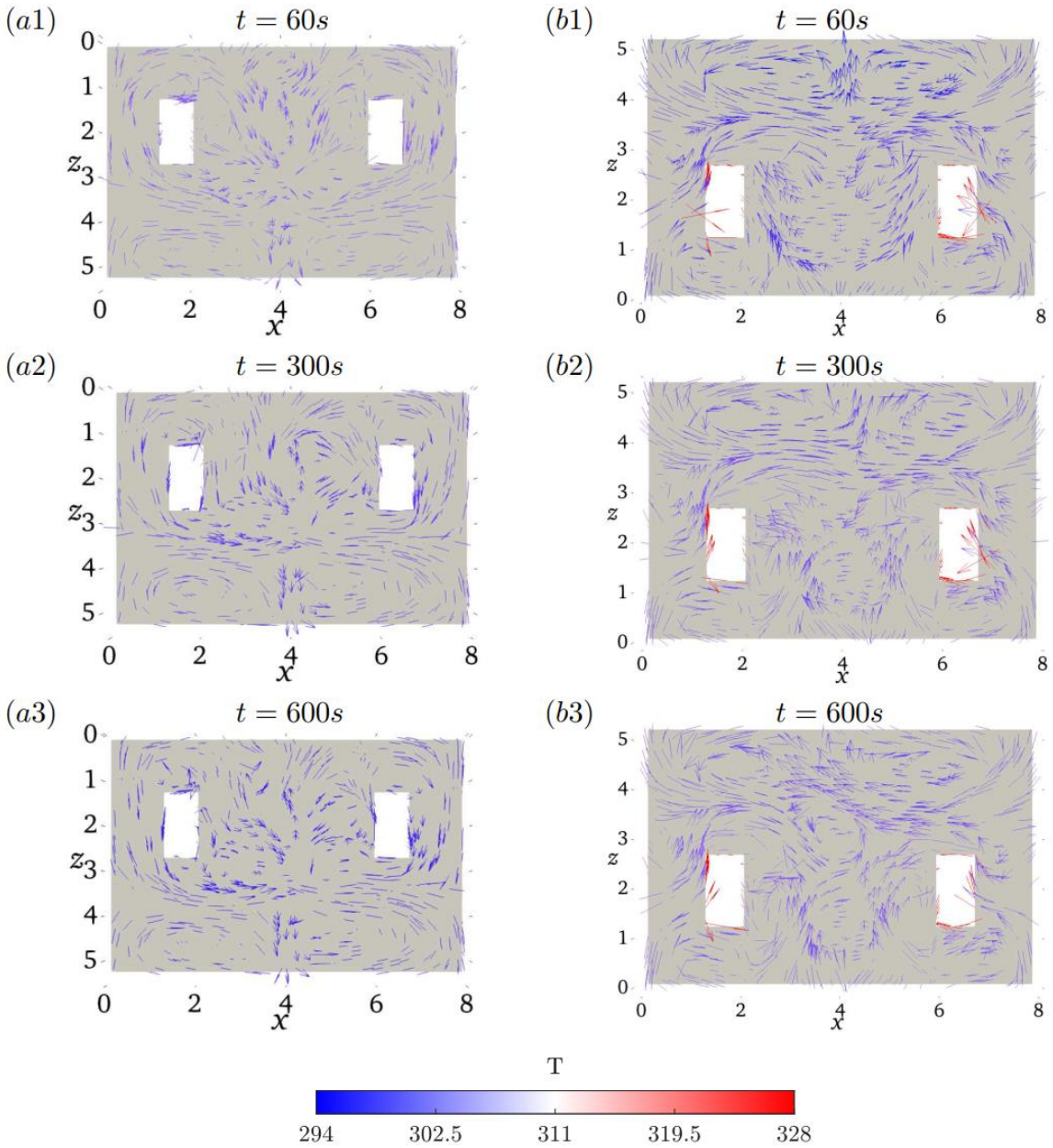

Fig. 11. Slice of velocity streamlines plot at $L_{y=}$1.5m coloured by temperature for at respective time for (a) Case 0 (b) Case 3

3.2 Effect of Air Ventilation with Operating Air Conditioner

The efficiency of air ventilation and/or air conditioner to achieve human comfort temperature in the room with different quantity of heat source in this section. Case 1 and 2 is simulated with a heat source and two heat sources is enabled in Case 4 and 5.

Figure 12 and Figure 13 shows the temperature contour of the room at t = 60s, 300s and 600s. In all cases, the air conditioner is running with cold air (294K) supplied. The effects of with (case 1 and 4) and without (case 2 and 5) turning on the air ventilation on the quantity of heat sources are investigated. The temperature contour in Case 2 and 5 (see Figure 13(b) and Figure12(b)) have darker colour indicates the temperature is lower compared to Case 1 and 4 (see Figure 13(a) and Figure12(a)). The ambient temperature reaches the steady state where T = T_{ac} = 294K at t = 300s in Case 2 and 5. The temperature difference between Case 1 and 2 are approximately 3K at t = 600s in

Figure 12(a3) and Figure 12(b3). When both heat sources are enabled, the temperature difference between Case 4 and 5 increases to approximately 8K in Figure 13(a3) and Figure 13(b3).

The comparison of the contour in Case 2 and 5 at t = 600s shows that cold air able to reduce the ambient temperature and achieves human comfort temperature in the room despite the quantity of heat source increases in Case 5. However, the ambient temperature between Case 4 and 5 differ significantly as the quantity of heat source increases. The usage of the air ventilation system is to draw the hot air out of the room to maintain the human comfort temperature range. However, when the air ventilation system and air conditioner are switched on at the same time, the efficiency of systems are dropped compares to the case with an air conditioner is switched on. This may be due to the position of the air condition is closed to the air ventilation system (see Figure 3). The air ventilation system draws cold air out of the room and causes the drop of efficiency.

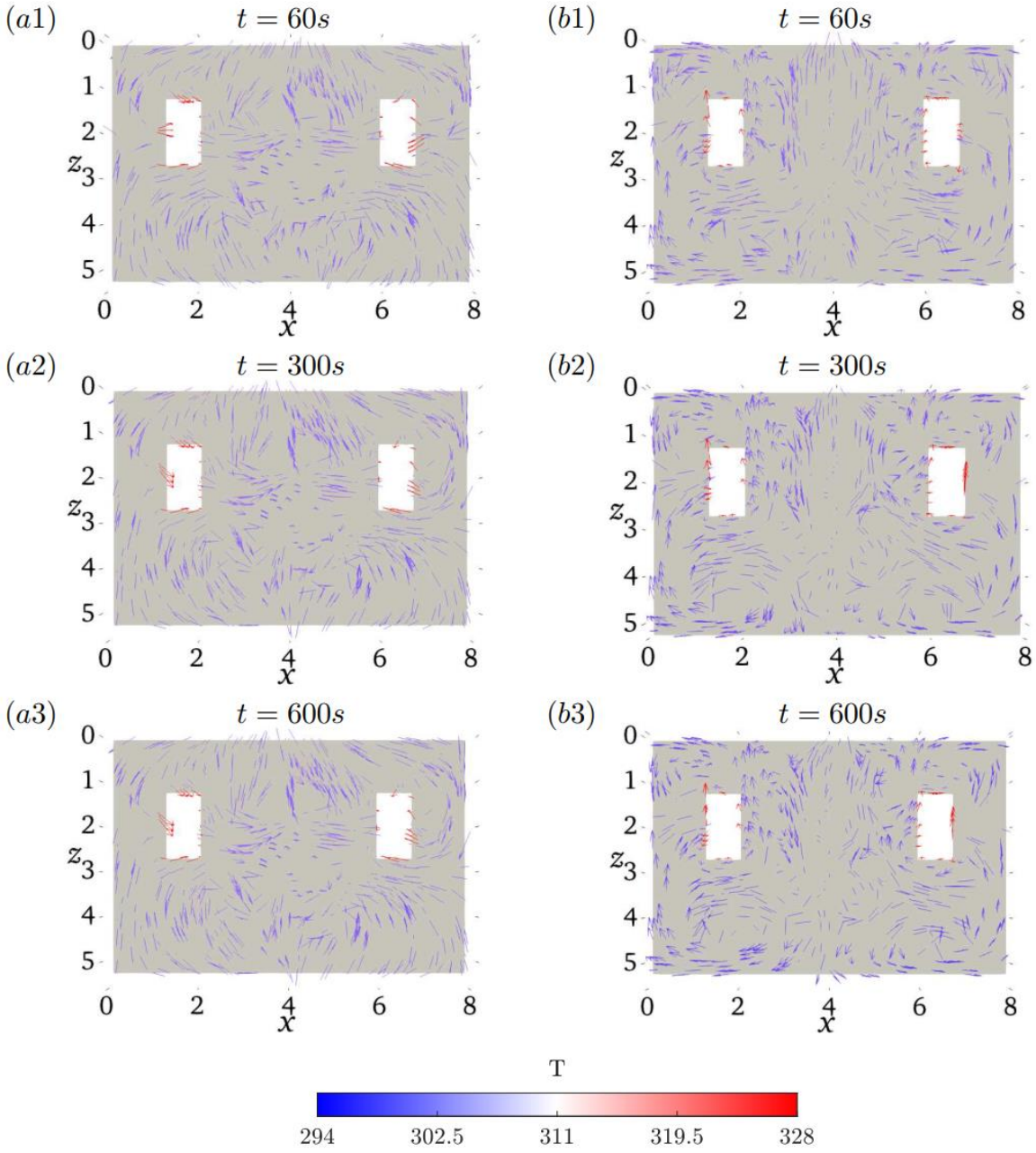

Fig. 12. Slice of velocity streamlines plot at L_y = 1.5m coloured by temperature for at respective time, t for (a) Case 1 (b) Case 2

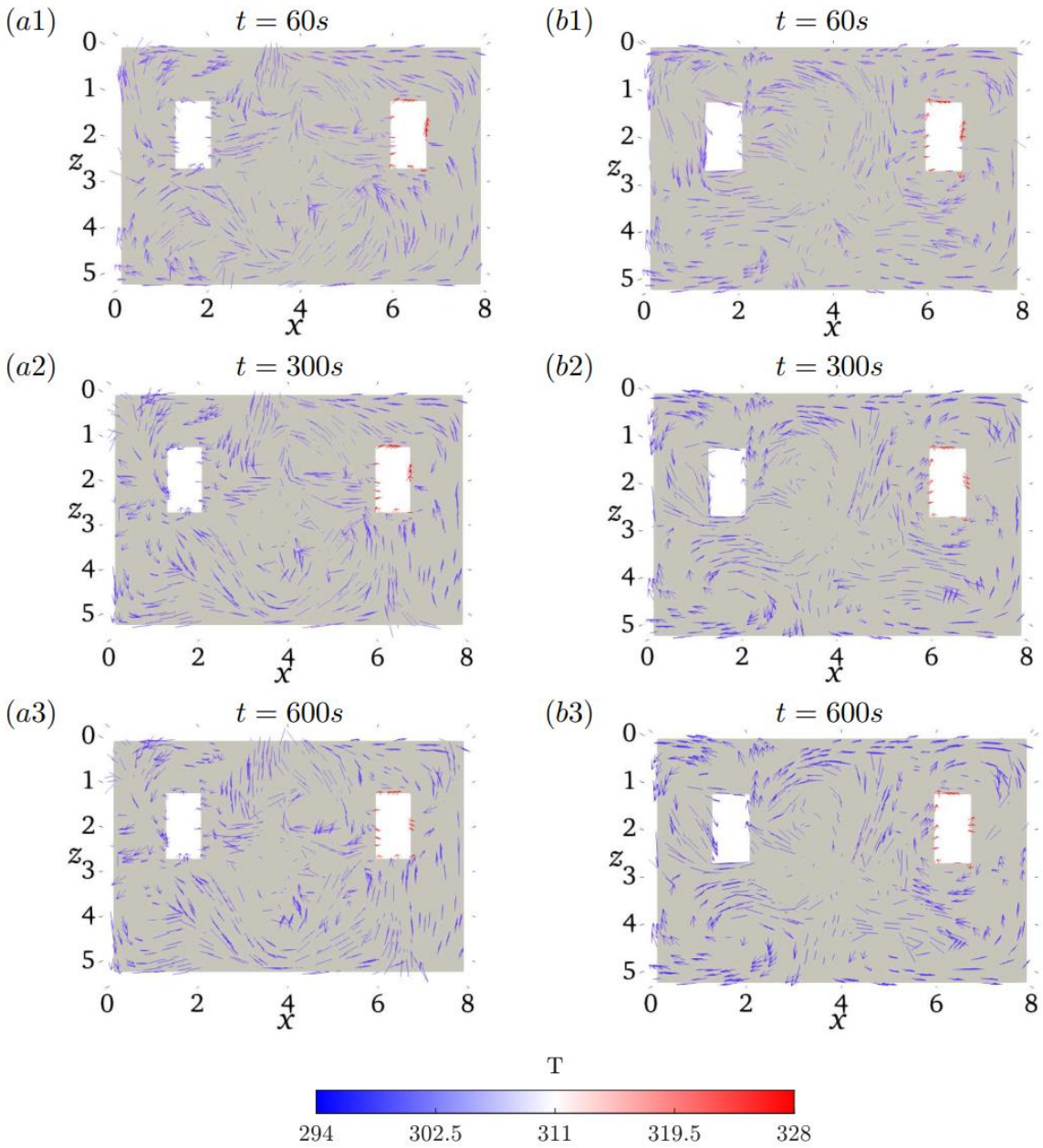

Fig. 13. Slice of velocity streamlines plot at L_y = 1.5m coloured by temperature for at respective time, t for (a) Case 4 (b) Case 5

3.3 Comparing the Importance of Air Conditioner and Air Ventilation System in Removing Heat

Air ventilation and temperature are crucial factors in thermal comfort. In this section, the performance between air ventilation and air conditioner is compared with two heat sources are enabled. In the first part, the air ventilation system is switched off. *PressureInletOutlet* velocity boundary condition is applied to the air conditioner. In the second part, the air ventilation system is switched off with cooling from the air conditioner.

Figure 14 shows the temperature contour of the room with Figure 14(a) air ventilation system and Figure 14(b) air conditioner is switched on. Both contours show the temperature reaches steady state at t = 300s. Case 3 achieves the steady state temperature at T = 305K and the steady state temperature of Case 5 is T ≤ 295K where it is close to temperature of cold air. The ambient

temperature for Case 3 increases from 298K to approximately 305K and it is significantly higher compared to Case 5.

The comparison shows that the air conditioner able to reduce and maintain the ambient temperature at the level of comfort. The air ventilation system able draws out the hot air around heat sources, however, the ambient temperature does not meet the level of comfort. Therefore, it can be concluded that the air conditioner able to reduce the temperature around the heat source and further reduce the ambient temperature.

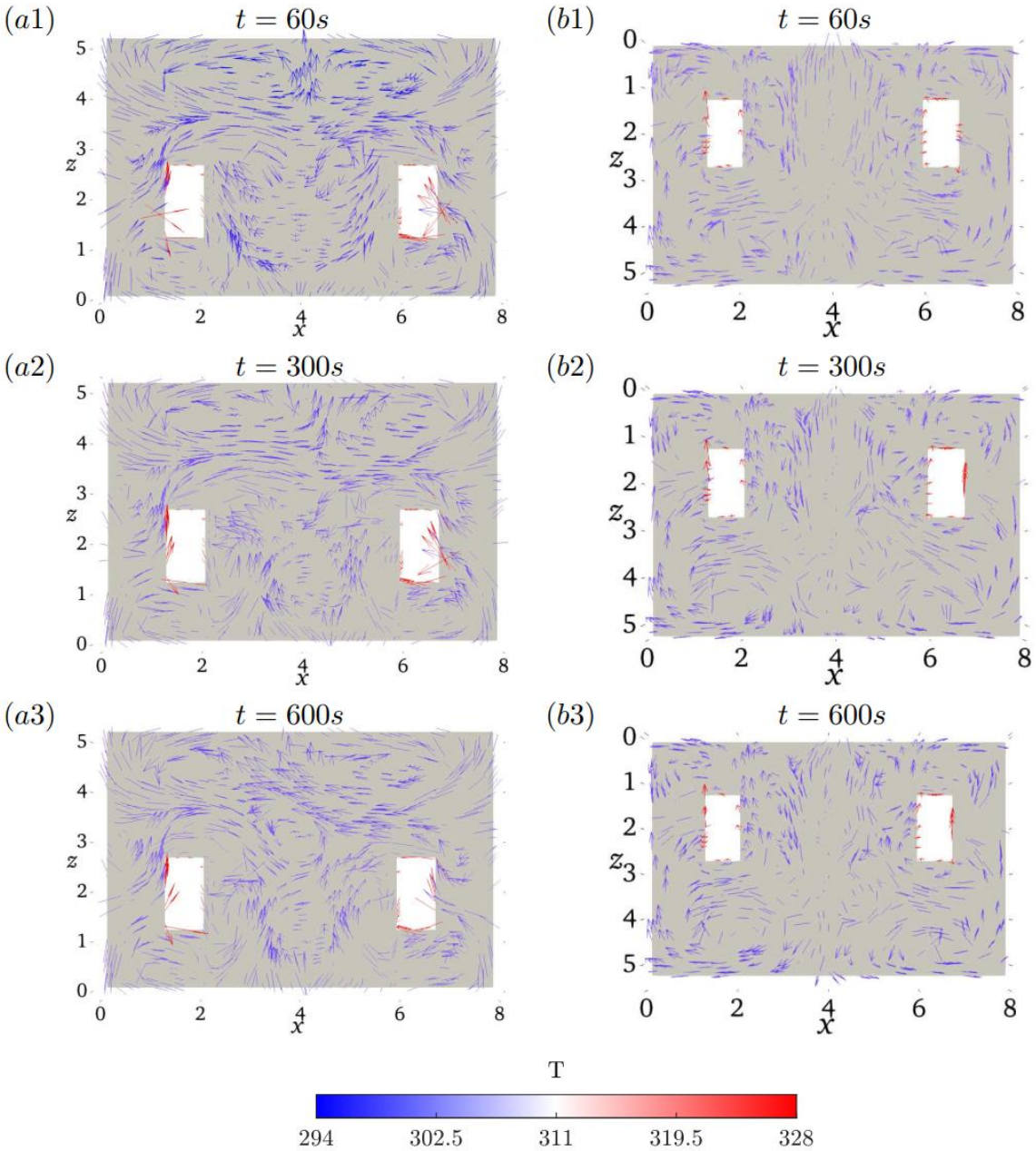

Fig. 14. Slice of velocity streamlines plot at L_y = 1.5m coloured by temperature for at respective time, t for (a) Case 3 (b) Case 5

4. Conclusion

Numerical simulation of ventilation in a confined space is simulated with various room conditions to investigate the air ventilation and heat transfer in a room. Different air recirculation pattern is observed in the temperature contour with velocity streamline plot for the case with air ventilation system is switched off with different quantity of heat source. Highest temperature is obtained in the case with extreme condition where the temperature increases up to 305K. Lowest temperature on the other hand is obtained in the case with relax condition where the temperature drops significantly and reaches steady state at the cold air temperature. The efficiency of systems reduces when both the air ventilation system and air condition are operating at the same time. This is due to the position of air conditioner is closed to the air ventilation system. Cold air is drawn out of the room before convective heat transfer is occurred. Hence, the temperature does not decrease significantly.

Acknowledgement

The authors would like to thank The Electricity Supply Industries Trust Account (AAIBE) for their financial support.

References

[1] Olesen, B. W., Domingo Moreno-Beltran, Mario Grau-Rios, E. Tahti, R. Niemela, L. Olander, and K. Hagstrom. "Target Levels. " Essay. In *Industrial Ventilation Design Guidebook*, 355–413. Elsevier, 2001. https://doi.org/10.1016/B978-012289676-7/50009-6

[2] Muhieldeen, M. W., and Y. C. Kuang. "Saving energy costs by combining air-conditioning and aircirculation using CFD to achieve thermal comfort in the building." *Journal of Advanced Research in Fluid Mechanics and Thermal Sciences* 58, no. 1 (2019): 84-99.

[3] Nielsen, Peter V. "Flow in air conditioned rooms." *(English translation of Ph. D. thesis from the Technical University of Denmark* (1976).

[4] Nielsen, Peter V., A. Restivo, and J. H. Whitelaw. "The velocity characteristics of ventilated rooms." (1978): 291-298. https://doi.org/10.1115/1.3448669

[5] Nielsen, Peter V., A. Restivo, and J. H. Whitelaw. "Buoyancy-affected flows in ventilated rooms." *Numerical Heat Transfer* 2, no. 1 (1979): 115-127. https://doi.org/10.1080/10407787908913402

[6] Daoud, Ahmed, and Nicolas Galanis. "Prediction of airflow patterns in a ventilated enclosure with zonal methods." *Applied energy* 85, no. 6 (2008): 439-448. https://doi.org/10.1016/j.apenergy.2007.10.002

[7] Omri, Mohamed, and Nicolas Galanis. "Evaluation of confined natural and forced convection predictions by different turbulence models." *International Journal of Numerical Methods for Heat & Fluid Flow* (2009). https://doi.org/10.1108/09615530910922125

[8] Zhang, Zhao, Wei Zhang, Zhiqiang John Zhai, and Qingyan Yan Chen. "Evaluation of various turbulence models in predicting airflow and turbulence in enclosed environments by CFD: Part 2—Comparison with experimental data from literature." *Hvac&R Research* 13, no. 6 (2007): 871-886. https://doi.org/10.1080/10789669.2007.10391460

[9] Zhu, Yiyun, Xiaona Fan, Changjiang Wang, and Guochen Sang. "Analysis of heat transfer and thermal environment in a rural residential building for addressing energy poverty." *Applied Sciences* 8, no. 11 (2018): 2077. https://doi.org/10.3390/app8112077

[10] Chanteloup, Vivian, and Pierre-Sylvain Mirade. "Computational fluid dynamics (CFD) modelling of local mean age of air distribution in forced-ventilation food plants." *Journal of Food Engineering* 90, no. 1 (2009): 90-103. https://doi.org/10.1016/j.jfoodeng.2008.06.014

[11] Buratti, C., R. Mariani, and Elisa Moretti. "Mean age of air in a naturally ventilated office: Experimental data and simulations." *Energy and Buildings* 43, no. 8 (2011): 2021-2027. https://doi.org/10.1016/j.enbuild.2011.04.015

[12] Benderradji, Razik, Hamza Gouidmi, Djedid Taloub, and Abdelhadi Beghidja. "Numerical study three-dimensional of mixed convection in a cavity: Influence of Reynolds and Grashof numbers." *Journal of Advanced Research in Fluid Mechanics and Thermal Sciences* 51, no. 1 (2018): 42-52.

[13] OpenFOAM, OpenFOAM User Guide. "The OpenFOAM Foundation." (2014).

[14] "A.1 Standard Solvers. " OpenFOAM. Accessed June 24, 2023. https://www.openfoam.com/documentation/user-guide/a-reference/a.1-standard-solvers.

[15] Limane, Abdelhakim, Hachimi Fellouah, and Nicolas Galanis. "Thermo-ventilation study by OpenFOAM of the airflow in a cavity with heated floor." In *Building simulation*, vol. 8, pp. 271-283. Tsinghua University Press, 2015. https://doi.org/10.1007/s12273-014-0205-4

[16] Fohimi, Nor Azirah Mohd, Muhammad Hanif Asror, Rosniza Rabilah, Mohd Mahadzir Mohammud, Mohd Fauzi Ismail, and Farid Nasir Ani. "CFD Simulation on Ventilation of an Indoor Atrium Space." *CFD Letters* 12, no. 5 (2020): 52-59. https://doi.org/10.37934/cfdl.12.5.5259

[17] Ismail, Mohd Azmi, and Mohd Sabri Che Jamil. "CFD HVAC study of modular badminton hall." *CFD Letters* 12, no. 7 (2020): 90-99. https://doi.org/10.37934/cfdl.12.7.9099